Journal of Non-Crystalline Solids 528 (2020) 119751

Contents lists available at ScienceDirect

Journal of Non-Crystalline Solids

journal homepage: www.elsevier.com/locate/jnoncrysol

Amorphous structure rejuvenation under cryogenic treatment of Al-based amorphous-nanocrystalline alloys

G. Abrosimova[a,*], N. Volkov[a], E. Pershina[a], Tran Van Tuan[b], A. Aronin[a,b,c]

[a] Institute of Solid State Physics RAS, Chernogolovka, Russia
[b] The National University of Science and Technology MISiS, Moscow, Russia
[c] National Research University Higher School of Economics, Moscow, Russia

ARTICLE INFO

Key words:
Cryogenic rejuvenation
Amorphous structure
Nanocrystals
Crystallization
Diffraction
Electron microscopy

ABSTRACT

Effect of cryogenic treatment on amorphous phase rejuvenation in Al-based alloys was studied by X-ray diffraction, transmission and high-resolution electron microscopy. It was established that cryogenic cycling may lead to amorphization of nanocrystalline regions and amorphous phase rejuvenation in partially crystalline samples. The composition of nanocrystals in the investigated samples differed from that of amorphous phase, therefore, the process of amorphization under cryogenic cycling was accompinied by mass transfer. A degree of amorphization depends on the duration of cryogenic cycling and increases with an increase in its duration. Amorphization of a partially crystalline structure under cryogenic cycling is observed for nanocrystals formed under both heat treatment and deformation.

1. Introduction

Amorphous and partially crystalline alloys are of a great interest due to their good physical and chemical properties. Al-based alloys are characterized by high yield strength, superior corrosion resistance and other desirable properties [1–4]. Fe- and Co-based alloys have a splendid combination of hysteresis properties, high values of saturation induction and effective permeability; depending on the composition they are characterized by high magnetic permeability and magnetic susceptibility. A number of these alloys have zero magnetostriction constant [5–6]. There are a lot of works devoted to the study of a structure of amorphous and partially crystalline alloys [7–9], specific features of phase transitions in these materials [10,11] and changes in physical properties caused by structural transformations [12,13]. Formation of a partially crystalline amorphous-nanocrystalline structure allows obtaining Al-based materials with high mechanical properties [14–18]. However, the possibilities of practical application of these materials are limited: the plasticity of alloys decreases under low-temperature annealing or just aging, they become brittle which significantly limits the areas of their potential applications in instruments and devices.

In a number of researches, attempts were made to recover plasticity by severe plastic deformation of samples [19–21]. In [21] it was shown that as a result of high-pressure torsion deformation changes in the pair distribution function of atoms were observed. This indicated that marked atomic restructurings caused by rejuvenation of an amorphous structure occur as a result of deformation. The authors of [21] assumed that these structural changes may be the result of local heating due to deformation. An increase in the degree of structure disordering under plastic deformation was noted also in [20,22]. A change of mechanical properties (hardness, modulus of elasticity, etc.) in $Zr_{50}Cu_{40}Al_{10}$ bulk metallic glass under severe plastic deformation was observed in [19].

However, it was found in recent years that plasticity can be recovered under thermal cycling in the temperature range between the temperature of liquid nitrogen and room or elevated temperature [23–25]. This process was called rejuvenation. A change in a structure under cryogenic thermal cycling is related to the following process. In an amorphous alloy there are heterogeneity regions which differ in the chemical compositions, density, short-range order degree, shear band, etc. In [25,26] a hypothesis was discussed that since such heterogeneity regions are characterized by different coefficients of thermal expansion, an abrupt change in temperature (heating ↔ cooling) will lead to the appearance of internal stresses which are capable of causing irreversible local atomic restructurings, thus, resulting in structure rejuvenation. At that rejuvenation of the structure in metallic glasses was linked to inhomogeneous values of the coefficient of thermal expansion in different sample regions (in the regions of intersection of shear bands, etc.). One of the examples of an increase in plasticity can be [23] the authors of which demonstrated recovery of the plasticity of $Zr_{55}Cu_{30}Al_{10}Ni_5$ bulk metallic glass under cryogenic cycling. However, the authors of [23]

* Corresponding author.
E-mail address: gea@issp.ac.ru (G. Abrosimova).

https://doi.org/10.1016/j.jnoncrysol.2019.119751
Received 15 August 2019; Received in revised form 16 October 2019; Accepted 23 October 2019
Available online 10 November 2019

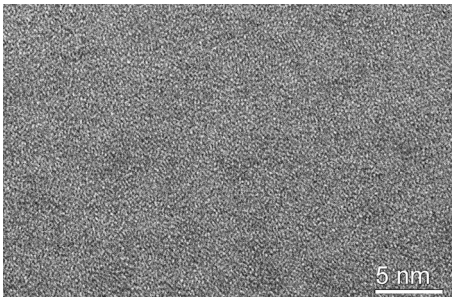

Fig. 1. High-resolution electron microscope image of initial $Al_{87}Ni_8Gd_5$ amorphous.

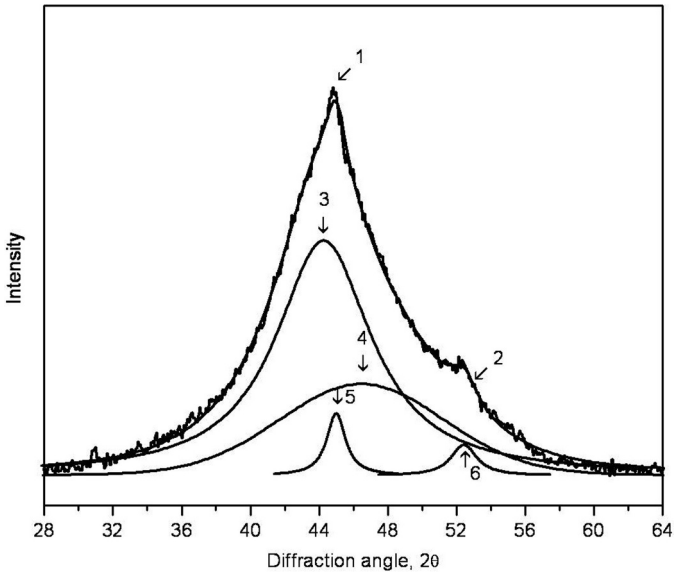

Fig. 2. Part of the X-ray diffraction patterns of annealed $Al_{87}Ni_8Gd_5$ sample (1 – experimental curve, 3 and 4 – diffuse halos from the first and second amorphous phases, 5 – diffraction peak from Al nanocrystals, 2 – summary of curves 3–6).

did not find changes in the structure under this treatment.

Note that a significant change in an amorphous structure has not been observed to date. At the same time, the idea of induction of stresses in a system with inhomogeneous distribution of the coefficients of thermal expansion seems to be very promising. One of the methods to test this hypothesis can be to create an initial structure with a possible greater difference in the coefficients of thermal expansion between different regions. The present works made an attempt of cryogenic cycling influence on an amorphous-nanocrystalline structure

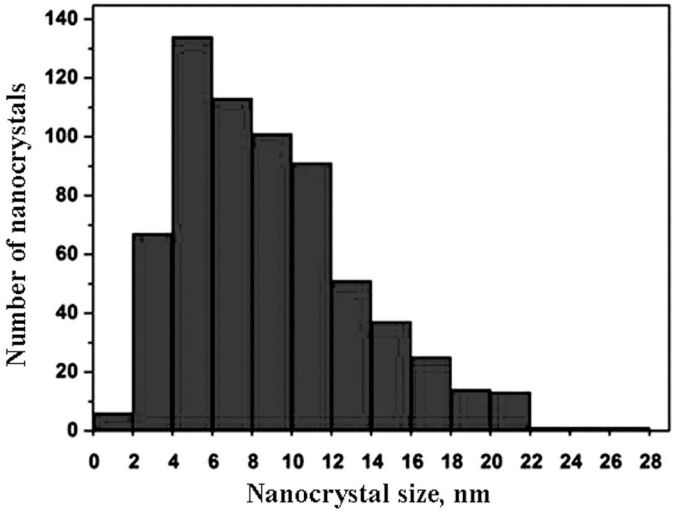

Fig. 4. Distribution of Al nanocrystals by size in annealed $Al_{87}Ni_6Gd_5$ alloy.

representing a system “amorphous matrix + nanocrystals” the components of which have a greater difference in the coefficients of thermal expansion than just different regions within an amorphous matrix.

2. Experimentals

Al-based amorphous alloys ($Al_{88}Ni_6Y_6$ and $Al_{87}Ni_8Gd_5$) were obtained in the form of ribbons by rapid melt quenching. The thickness of the ribbons was about 30 μm, the width was 1 cm. The amorphous samples were subjected to preliminary heat treatment in order to produce a partially crystalline structure, following which they were subjected to cryogenic cycling in the different temperature range (77 K - room temperature and 77–373 K). Under this treatment, the samples in a metal holder were placed to a container with liquid nitrogen, exposed at the temperature of liquid nitrogen during N s, removed from the container and exposed in the air at room temperature during N s. The duration of exposure in liquid nitrogen and in the air was similar and was from 30 s to 3 min, the number of these treatment cycles was from 30 to 200. The structure of the as-prepared and treated samples was investigated by X-ray diffraction and transmission electron microscopy. The X-ray diffraction studies were carried out on a Siemens D500 diffractometer using CoK_α radiation. To perform the X-ray diffraction studies, special substrates were used which do not give intrinsic reflections [27]. The use of soft Co K_α radiation enabled to stretch the X-ray diffraction pattern and, on the one hand, to see distortions of diffuse maxima more clearly, and, on the other hand, to determine their location more precisely. The fraction of the nanocrystalline phase was

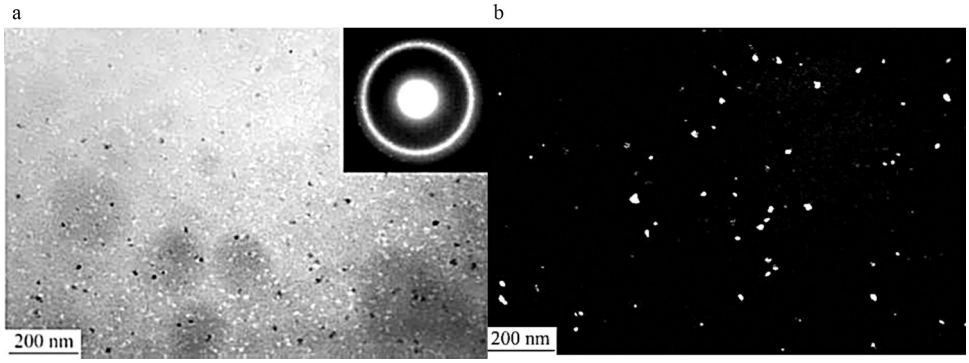

Fig. 3. Bright-field (*a*) and dark-field (*b*) TEM images of annealed $Al_{87}Ni_8Gd_5$ alloy and electron diffraction pattern (inset).

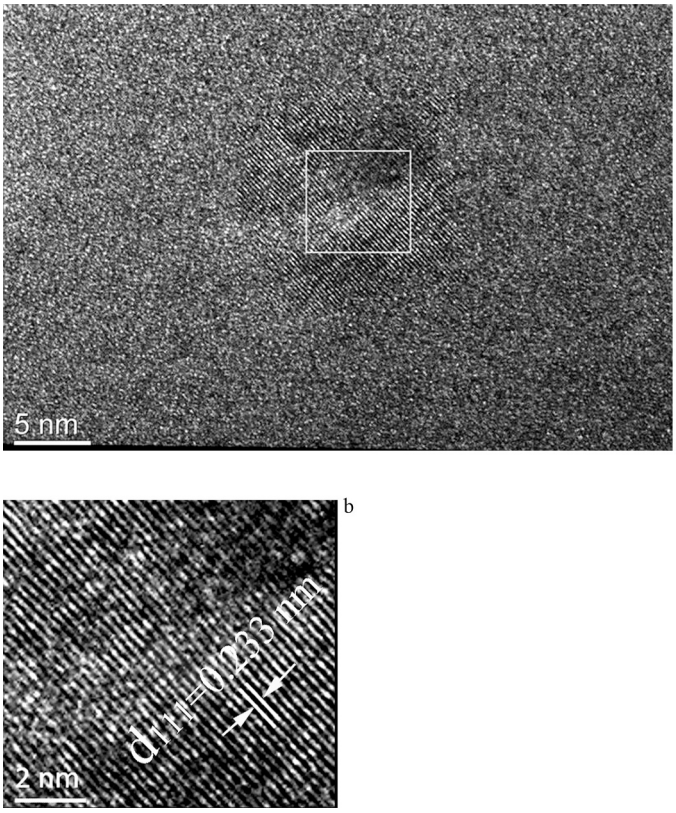

Fig. 5. High-resolution electron microscope image (a) and enlarged image of the region limited by a box (b) of Al nanocrystal in the amorphous matrix of $Al_{87}Ni_8Gd_5$ alloy.

determined by the ratio of integral intensities of the phases according to [28–30]. All the X-ray diffraction patterns were recorded at room temperature after completion of the cryogenic thermal cycling process. Up to the beginning of the structural researches the samples were stored in liquid nitrogen and removed take out immediately before the beginning of the recording of X-ray diffraction patterns. The foils for electron microscopic investigations were obtained by ion thinning. The calorimetric studies were carried out on a Perkin Elmer DSC-7 differential scanning calorimeter at a heating rate of 20 K/min. The electron microscopic studies were performed on JEM-100 CXII and JEM 2100 transmission electron microscopes.

3. Results

3.1. Evolution of the structure of $Al_{87}Ni_8Gd_5$ amorphous alloy

After quenching all ribbons were amorphous. Fig. 1 shows a high-resolution electron microscopy image of the as-prepared amorphous alloy. For the formation of a partially crystalline (amorphous-nanocrystalline) structure, the samples were annealed at 373–443 K during 1–5 h. Fig. 2 illustrates an X-ray diffraction pattern of $Al_{87}Ni_8Gd_5$ alloy after 1-hour annealing at 443 K (curve 1). It is seen that the diffuse maximum is non-symmetric and represents a superposition of two diffuse maxima (curves 3 and 4) and two diffraction reflections (curves 5 and 6). Curve 3 corresponds to the amorphous phase with a large radius of the first coordination sphere; this amorphous phase is enriched in gadolinium (the largest atom in the system under study). The amorphous phase characterized by a smaller radius of the first coordination sphere (curve 4) corresponds to the phase depleted in gadolinium and enriched in nickel. Curves 5 and 6 represent (111) and (200) diffraction reflections from the fcc phase. Curve 2 represents a sum of curves 3 - 6. Thus, after annealing the structure of the samples represents a heterogeneous amorphous phase with nanocrystals randomly distributed in it. The heterogeneous amorphous phase in Al-based amorphous alloys after heat treatment and deformation was observed earlier [31–34]. The released nanocrystals are precipitations of pure aluminum; neither nickel nor gadolinium dissolves in Al lattice [35]. At the analysis of the diffuse maximum the values of half-widths of amorphous phase Gaussians and the position of aluminum reflections were taken into consideration [36–38]. The average nanocrystal size is about 10 nm.

Fig. 3 demonstrates a microstructure of annealed $Al_{87}Ni_8Gd_5$ alloy. In a bright-field (*a*) and dark-field (*b*) images one can see nanocrystals in the amorphous matrix. In an electron diffraction pattern (inset in Fig. 3a) one can see point reflections from the nanocrystals in a diffuse ring. Distribution of the nanocrystals by size in the annealed alloy is shown in Fig. 4. The average nanocrystal size is 10 nm which corresponds to the data of the X-ray diffraction studies. Fig. 5 demonstrates a high-resolution electron microscope image of Al nanocrystal in the amorphous matrix of $Al_{87}Ni_8Gd_5$ alloy after annealing. In the image there are nanocrystals formed during heat treatment, one of them being shown by a box. Note that the nanocrystal does not contain linear defects. Such defect-free nanocrystals in Al-based alloys were observed earlier [10].

The annealed samples with an amorphous-nanocrystalline structure were subjected to cryogenic thermal cycling in the temperature range of 77–373 K. A decrease in the fraction of the nanocrystalline phase was observed after 50 cycles of treatment. A decrease in the fraction of the nanocrystalline phase was observed under both X-ray diffraction and electron microscopic studies. The average nanocrystal size did not change at that. Fig. 6 illustrates a bright-field (a) and dark-field (b) electron microscope images of the sample structure after 100 cycles of treatment. Fig. 7 shows distribution of the nanocrystals by size.

A decrease in the fraction of the nanocrystalline phase became apparent in the X-ray diffraction patterns in a decrease in the intensity of the diffraction maxima (curves 5, 6) in Fig. 8 compared to the intensity of the diffraction reflections in Fig. 2 (curves 5, 6). Nanocrystals are

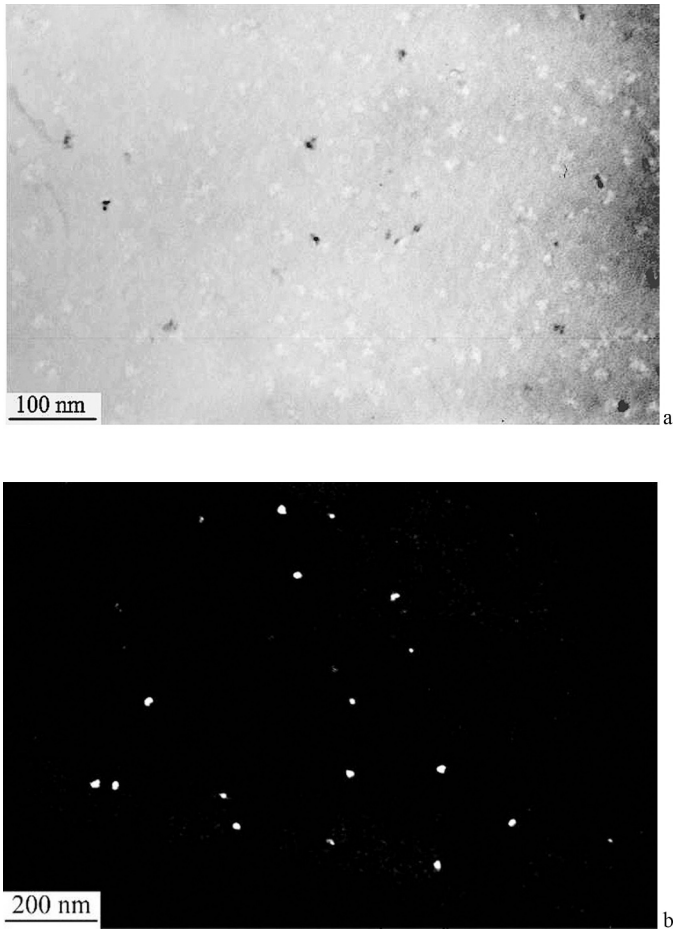

Fig. 6. Bright-field (a) and dark-field (b) electron microscope images of the sample structure after 100 cycles of treatment.

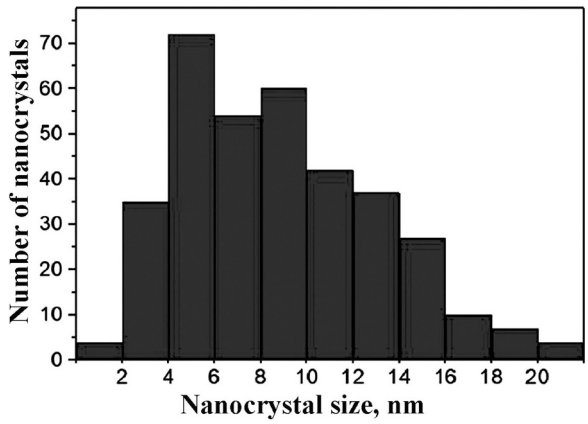

Fig. 7. Distribution of nanocrystals by size after cryogenic thermal cycling.

found more rarely in the electron microscope images of the samples after cryogenic cycling. At the similar number of the images obtained, under the similar conditions the total number of the observed nanocrystals after cryogenic cycling is less than that before it. This is indicated, in particular, in the histograms of distribution by size: the number of crystals (coordinate axis) in the samples after cryogenic cycling (Fig. 7) is less than that before cryogenic cycling (Fig. 4).

Since the method of transmission electron microscopy is local, a rarer location of nanocrystals may be accidental, and a thickness of the foil in the area under study may be less. Additional experiments were carried out to test the observed effect. The additional investigations

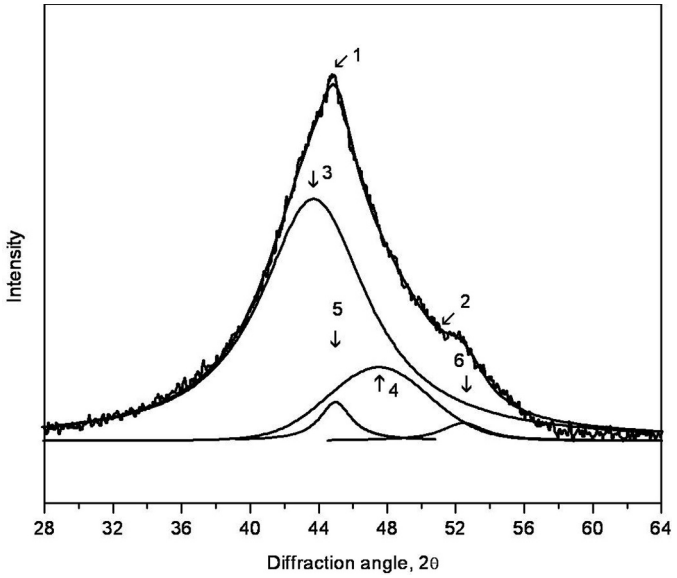

Fig. 8. Part of the X-ray diffraction pattern of $Al_{87}Ni_8Gd_5$ sample after annealing and cryogenic cycling (100 cycles) (1 – experimental curve, 3 and 4 – diffuse reflections from two amorphous phases, 5 and 6 – reflections from Al nanocrystals, 2 – summary of curves 3–6).

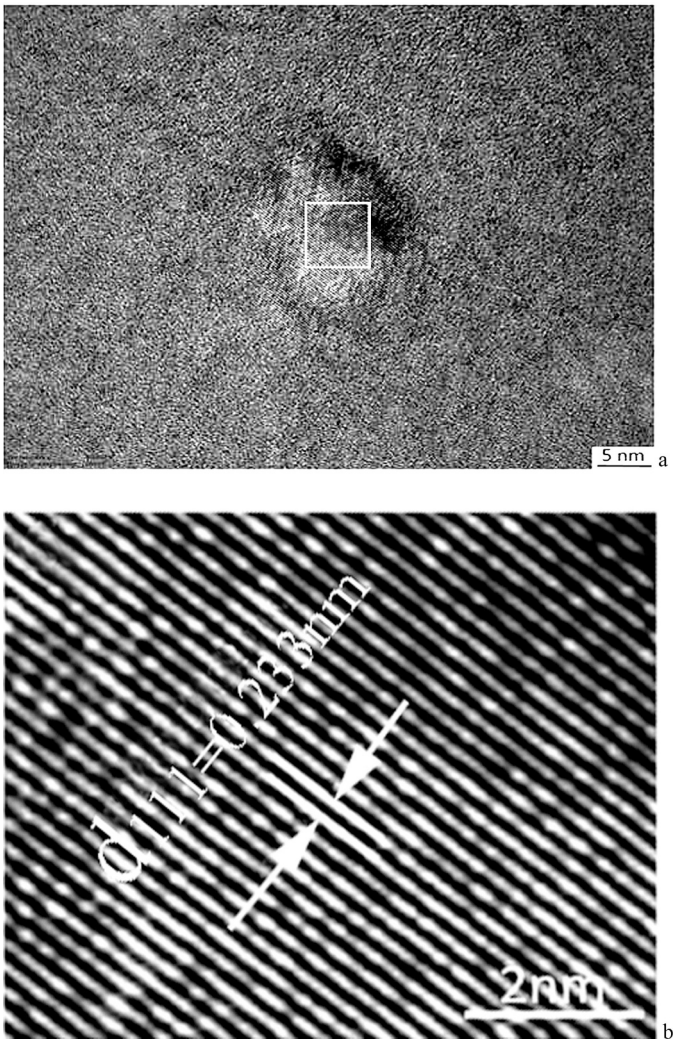

Fig. 9. High-resolution electron microscope image (a) and enlarged image of the region limited by a box (b) of Al nanocrystal in $Al_{87}Ni_8Gd_5$ alloy after thermal cycling.

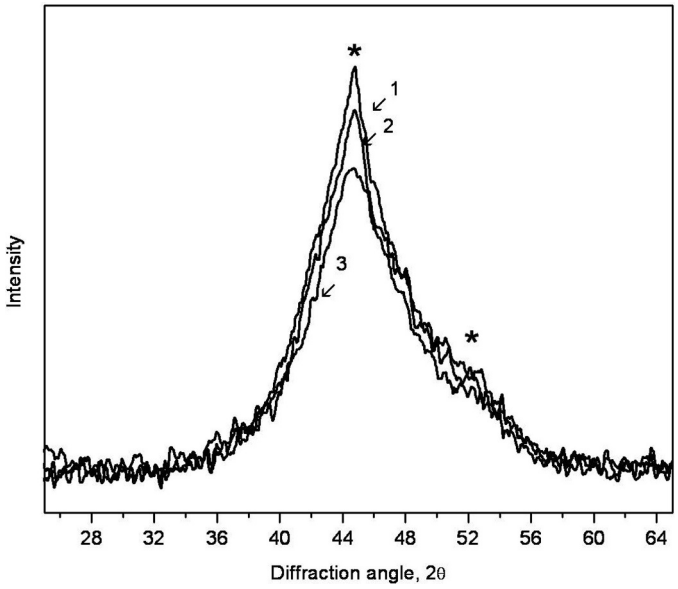

Fig. 10. X-ray diffraction patterns of samples after annealing (1) and cryogenic cycling (2 – 100 cycles, 3 – 200 cycles).

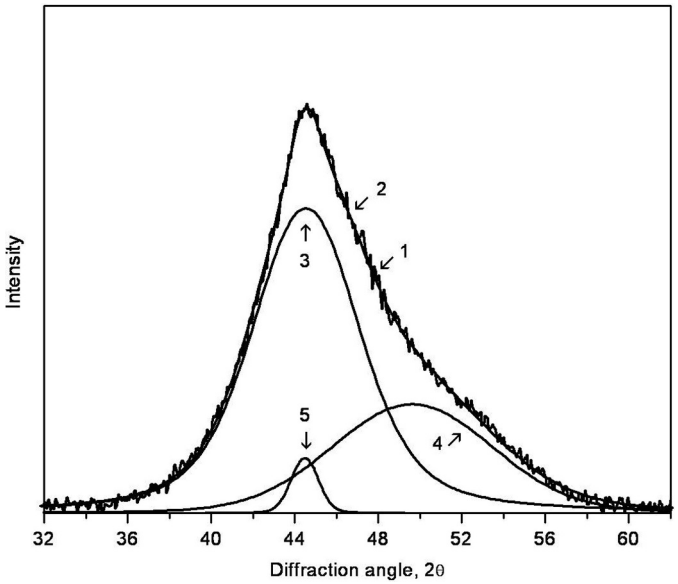

Fig. 11. Part of the X-ray diffraction pattern of deformed $Al_{88}Ni_6Y_6$ alloy (1 – experimental spectrum, 3 and 4 – diffuse reflections from two amorphous phases, 5 and 6 – reflections from Al nanocrystals, 2 – summary of curves 3–6).

were performed on the samples which had the similar absorption contrast ratio, i.e., the similar thickness. The results of the investigations showed that indeed the number of nanocrystals in the samples after thermal cycling is less than that in the annealed sample before cryogenic thermal cycling. At that, a significant change in distribution of the crystals by size after thermal cycling was not observed.

Fig. 9 presents a high-resolution electron microscope image of Al nanocrystal after thermal cycling. As it is seen, nanocrystals remain defect-free after this treatment.

As cryogenic cycling continues, the fraction of the nanocrystalline phase goes on decreasing. Fig. 10 demonstrates X-ray diffraction patterns of the annealed sample (1) and the samples after cryogenic cycling (2–100 cycles, 3–200 cycles). The reflections from aluminum nanocrystals are marked by asterisks. One can see that the intensity of the most intense Al (111) reflection reduced significantly after cryogenic cycling. According to the data of the X-ray diffraction study, the samples are completely amorphous after 200 cycles of treatment.

3.2. Evolution of the structure of $Al_{88}Ni_6Y_6$ amorphous alloy

Changes in an amorphous-nanocrystalline structures were made also in $Al_{88}Ni_6Y_6$ alloy, however, in contrast to $Al_{87}Ni_8Gd_5$ alloy the partially crystalline structure in $Al_{88}Ni_6Y_6$ alloy was produced by deformation. The amorphous samples were deformed by multiple rolling at room temperature. The value of deformation was ~50%. An initial section of the X-ray diffraction pattern of the deformed sample is illustrated in Fig. 11. As well as in the case of annealing, after deformation the amorphous phase is heterogeneous and contains regions differing in the chemical composition (diffuse halos 3 and 4) and a small amount of nanocrystals (curve 5). In this alloy, yttrium atom is the largest one; the phase corresponding to the left diffuse subpeak is enriched in this component. Accordingly, the second amorphous phase (curve 4) is depleted in it. The average size of Al nanocrystals determined by the Selyakov-Scherrer formula [39] is 6 nm.

An image of the structure of $Al_{88}Ni_6Y_6$ alloy after deformation is shown in Fig. 12. The structure of the rolled sample consists of an amorphous phase with a small amount of nanocrystals. According to the data of the electron microscopic study, the average nanocrystal size is also 6 nm.

The deformed samples of $Al_{88}Ni_6Y_6$ alloy were subjected to cryogenic cycling similarly to the annealed samples of $Al_{87}Ni_8Gd_5$ alloy. As well as in the case of the alloy with Gd, cryogenic cycling leads to a significant decrease in the fraction of the nanocrystalline phase. Fig. 13 shows an X-ray diffraction pattern of deformed $Al_{88}Ni_6Y_6$ alloy after cryogenic cycling in the temperature range of 77–373 K (60 cycles). With an increase in the number of cycles to 100 and more no signs of the crystalline phase were observed in the X-ray diffraction pattern.

A comparison of the X-ray diffraction patterns in Figs. 11 and 13 demonstrates unambiguously a significant decrease in the fraction of crystals in the sample after cryogenic cycling. We estimate that after this treatment the fraction of the nanocrystalline phase decreased approximately by 6 times. A microstructure of the sample after cryogenic cycling is shown in Fig. 14 where one can clearly see a decrease in the amount of nanocrystals.

The similar results were obtained also under cryogenic cycling in the temperature range of 77–273 K. Thus, in both of the partially crystalline alloys cryogenic cycling leads to reduction and/or disappearance of the crystalline phase, i.e., structure rejuvenation.

4. Discussion

The obtained results demonstrate that under cryogenic cycling a decrease in the fraction of the crystalline phase occurs, i.e., nanocrystals amorphize. The works on investigation of the transition from the crystalline to the amorphous state (for example, under deformation) were carried out earlier [40,41]. One of these examples can be the investigation of Ni-Ti alloys where amorphization of the crystalline phase occurred due to the martensite transformation without a change in the chemical composition. In the studied alloys the transition from the crystalline to the amorphous state (“dissolution” of nanocrystals) occurs by the other mechanism. As noted above, nanocrystals in the investigated alloys represent precipitations of pure aluminum, whereas the amorphous matrix is three-component. Consequently, during cryogenic cycling not only system disordering, but also component redistribution occurs. Apparently, the observed change in the structure is initiated by the stresses caused by thermal gradients between the neighboring regions in the heterogeneous structure, difference in the coefficients of thermal expansion. As shown above, the heterogeneous amorphous structure in the investigated alloys is formed after both annealing and deformation, with nanocrystals and heterogeneous amorphous structure being formed in both of the cases.

To estimate thermotension arising at temperature change one can

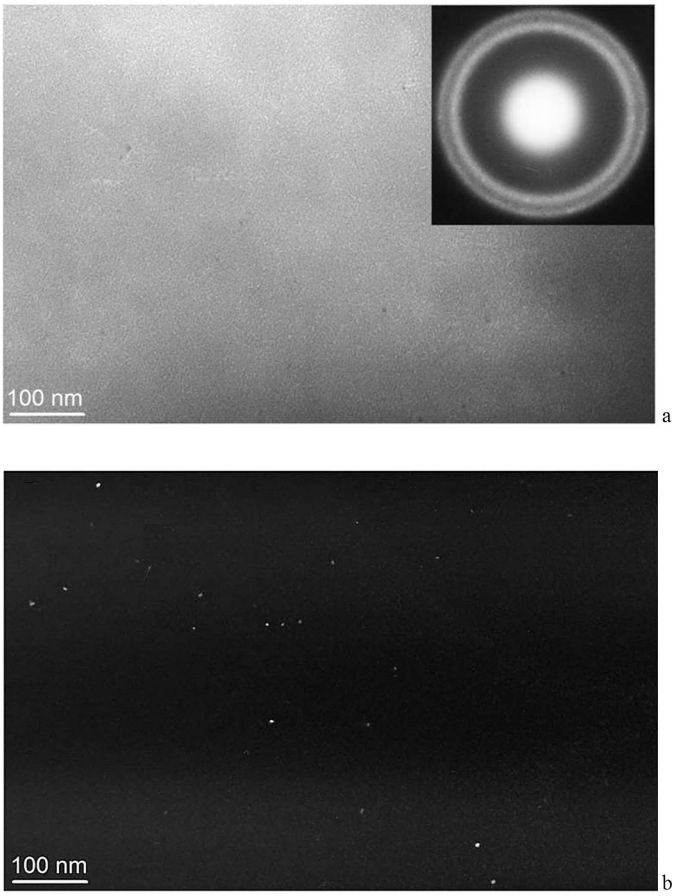

Fig. 12. Bright-field (a) and dark-field (b) TEM images of the structure of deformed $Al_{88}Ni_6Y_6$ alloy.

use the Selsing model [42] which is described by the formula:

$$\sigma_p = \frac{\Delta\alpha \cdot \Delta T}{\frac{1+\nu_m}{2E_m} + \frac{1-2\nu_p}{2E_p}}, \quad (1)$$

where σ_p is the average stress inside particles;

$\Delta\alpha$ is the difference in the coefficients of thermal expansion of particles and a matrix;

ν_m and ν_p are the Poisson's ratios of a matrix and particles;

E_m and E_p are the Young's moduli of a matrix and particles, respectively.

The average stress σ_m in a matrix is determined by the equation:

$$f \cdot \sigma_p + (1-f) \cdot \sigma_m = 0. \quad (2)$$

Eq. (1) shown above works in the case when the volume fraction of second phase particles does not exceed 10%. The general formula with regard to the fraction of particles f has the form [42]:

$$\sigma_p = \frac{\Delta\alpha \cdot \Delta T}{\frac{1}{3K_p} + \frac{1}{4(1-f)G_m} + \frac{f}{3(1-f)K_m}}, \quad (3)$$

where K_p, K_m are the bulk moduli of particles and a matrix, respectively; G_m is the shear modulus of a matrix.

From Eqs. (2) and (3) it follows that stresses inside particles and in a matrix have opposite signs. That means that if there is tensile stress in particles, there is compressive stress in a matrix, and conversely. Stress inside particles by the absolute value decreases approximately by the linear law with an increase in particle fraction, whereas stress in a matrix increases.

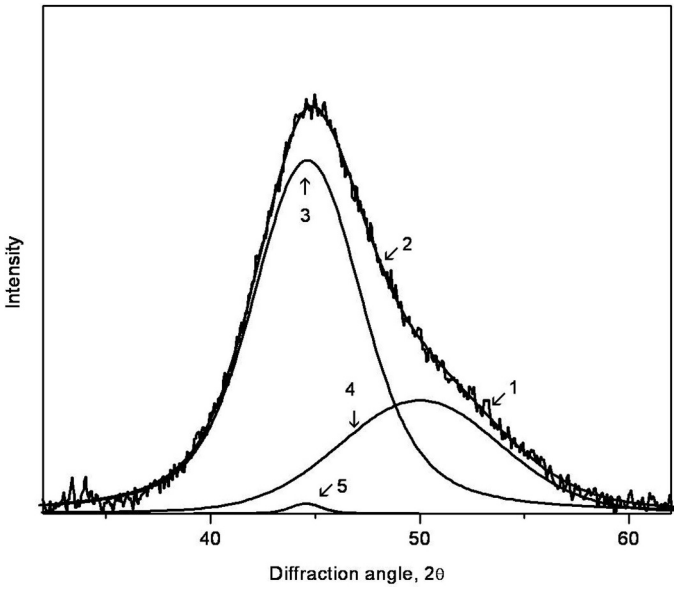

Fig. 13. Part of the X-ray diffraction pattern of deformed $Al_{88}Ni_6Y_6$ alloy (1 – experimental spectrum, 3 and 4 – diffuse reflections from two amorphous phases, 5 and 6 – reflections from Al nanocrystals, 2 – summary of curves 3–6).

Since according to the data of the X-ray diffraction studies the amount of the crystalline phase did not exceed a few percent, Eq. (1) was used for the subsequent estimations. The mechanical characteristics for Al and the amorphous matrix in the case of $Al_{87}Ni_8Gd_5$ alloy, which were used for the calculations of thermotension, are presented in Table 1.

The calculation result shows that in the case of $Al_{87}Ni_8Gd_5$ alloy the stress inside Al nanocrystals may reach 90 MPa under a change in the temperature in the range of 77–393 K. Due to heterogeneity of the amorphous matrix this stress has both normal and shear components and cannot be considered as a hydrostatic one.

The stress of dislocation generation τ according to the Frank-Read source can be estimated in the first approximation as corresponding to the equation:

$$\tau = \frac{Gb}{L}, \quad (4)$$

where G is the shear modulus; b is the modulus of Burgers vector; L is the nanocrystal size.

Such defects as twins and stacking faults [46] usually arise most frequently in nanocrystals. Passage of partial Shockley dislocations with the Burgers vectors $a/6<121>$ in Al nanocrystals is necessary for the formation of twins and stacking faults in them. According to Eq. (4), at $L = 10$ nm stress of about 450 MPa is necessary for the formation of such a dislocation. This stress turns to be much larger than that estimated by the Selsing formula for thermotensions arising inside nanocrystals. However, the calculation did not take into account cyclical influence on the material and rate of temperature change. Assuming that stresses increase with an increase in the number of cycles (or that the stress of dislocation generation decreases under cyclic load), that may lead to the occurrence of dislocations in nanocrystals and basically to their deformation amorphization.

As it was mentioned above, deformation amorphization is known in principle [40,41] however amorphization investigated in [40,41] occurred without concentration redistribution. The distinction of the present work is also in the fact that due to different compositions of the amorphous and crystalline phases amorphization should be accompanied by mass transfer. It is also important to note that in Al-based alloys the amorphous matrix is heterogeneous [10,38], the presence of

a

b

Fig. 14. Bright-field (a) and dark-field (b) TEM images of the structure of deformed $Al_{88}Ni_6Y_6$ alloy after cryogenic cycling (60 cycles).

Table 1
Elastic constants of Al and the amorphous matrix.

Phase	Coefficient of thermal expansion, 10^{-6} K^{-1}	Poisson's ratio	Young's modulus, GPa	References
Al	23.30	0.31	72	[43]
Matrix	11.07	0.28	20	[44,45]

heterogeneities with different coefficients of thermal expansions will also contribute to the occurrence of thermotensions in the material. In different areas the value of thermally induced stress, of course, turns to be different.

Apparently, additional experiments are necessary to establish definitively the mechanism of nanocrystal amorphization under thermal cycling.

5. Conclusion

It has been shown that application of cryogenic cycling actually to partially crystalline samples may result in amorphization of nanocrystalline regions and rejuvenation of an amorphous phase. Amorphization of the partially crystalline structure occurs both when nanocrystals were formed under heat treatment and in the case of their formation during deformation. The composition of nanocrystals differs from that of amorphous phases, that is why the process of amorphization under cryogenic cycling is accompanied by mass transfer. The degree of amorphization depends on the duration of cryogenic cycling and increases with an increase of its duration.

Declaration of Competing Interest

The authors declare that they have no known competing financial interests or personal relationships that could have appeared to influence the work reported in this paper.

Acknowledgements

The research is carried out within the state task of ISSP RAS and partially supported by the RFBR (grant no. 19-03-00355).

References

[1] J.H. Perepezko, Nucleation-controlled reactions and metastable structures, Prog. Mater. Sci. 49 (2004) 263–284 https://doi.org/10.1016/S0079-6425(03)00028-8.
[2] J. Mu, H. Fu, Z. Zhu, A. Wang, H. Li, Z.Q. Hu, Haifeng Zhang, Synthesis and properties of Al-Ni-La bulk metallic glass, Adv. Eng. Mater. 11 (2009) 530–532, https://doi.org/10.1002/adem.200900100.
[3] B.J. Yang, J.H. Yao, Y.S. Chao, J.Q. Wang, E. Ma, Developing aluminum-based bulk metallic glasses, Phil. Mag. 90 (2010) 3215–3231, https://doi.org/10.1080/14786435.2010.484401.
[4] S.Z. Du, C.C. Li, S.Y. Pang, J.F. Leng, H.R. Geng, Influences of melt superheat treatment on glass forming ability and properties of Al84Ni10La6 alloy, Mater. Des. 47 (2013) 358–364, https://doi.org/10.1016/j.matdes.2012.12.002.
[5] V.J. Chunchu, G. Markandeyulu, Magnetoimpedance studies in as quenched $Fe_{73.5}Si_{13.5}B_8CuV_{3-x}AlNb_x$ nanocrystalline ribbons, Appl. Phys. 113 (2013) 17A321, https://doi.org/10.1063/1.4795800.
[6] R. Xiang, Sh. Zhou, B. Dong, G. Zhang, Z. Li, Y. Wang, Ch. Chang, Effect of Co addition on crystallization and magnetic properties of FeSiBPC alloys, Progr. In Natural Sci. Mater. Intern. 24 (2014) 649–654, https://doi.org/10.1016/j.pnsc.2014.10.002.
[7] G.E. Abrosimova, A.S. Aronin, E. Yu, Ignat'eva, V.V. Molokanov, Phase decomposition and nanocrystallization in amorphous Ni70Mo10P20 alloy, JMMM 203 (1999) 169–171, https://doi.org/10.1016/S0304-8853(99)00216-4.
[8] D.V. Louzguine, A. Inoue, Comparative study of the effect of cold rolling on the structure of Al–Re–Ni–Co (RE = rare-earth metals) amorphous and glassy alloys, J. Non-Cryst. Solids 352 (2006) 3903–3908, https://doi.org/10.1016/j.jnoncrysol.2006.06.022.
[9] A.S. Aronin, G.E. Abrosimova, Yu.V. Kir'yanov, Formation and structure of nanocrystals in an $Al_{86}Ni_{11}Yb_3$ alloy, Physics of the Solid State 43 (2001) 2003–2011, https://doi.org/10.1134/1.1417170.
[10] G.E. Abrosimova, A.S. Aronin, E. Yu, Ignat'eva, mechanism of crystallization of the $Ni_{70}Mo_{10}B_{20}$ alloy above the glass transition temperature, Physics of the Solid State 48 (2006) 563–569, https://doi.org/10.1134/S1063783406030243.
[11] N. Boucharat, R. Hebert, H. Rosner, R. Valiev, G. Wilde, Nanocrystallization of amorphous $Al_{88}Y_7Fe_5$ alloy induced by plastic deformation, Scr. Mater. 53 (2005) 823–828, https://doi.org/10.1016/j.scriptamat.2005.06.004.
[12] B.-G. Yoo, Y.-J. Kim, J.-H. Oh, U. Ramamurty, J. Jang, On the hardness of shear bands in amorphous alloys, Scr. Mater. 61 (2009) 951–954, https://doi.org/10.1016/j.scriptamat.2009.07.037.
[13] A. Concustell, G. Alcalá, S. Mato, T.G. Woodcock, A. Gebert, J.Eckert A., M.D. Baró, Effect of relaxation and primary nanocrystallization on the mechanical properties of $Cu_{60}Zr_{22}Ti_{18}$ bulk metallic glass, Intermetallics 13 (2005) 1214–1219, https://doi.org/10.1016/j.intermet.2005.04.003.
[14] Y.H. Kim, A. Inoue, T. Masumoto, Increase in mechanical strength of al-y-ni amorphous alloys by dispersion of nanoscale fcc-Al particles, Mater. Trans. J I M 32 (1991) 331–338, https://doi.org/10.2320/matertrans1989.32.331.
[15] J. Eckert, M. Calin, L.C. Zhang, S. Scudino, C. Duhamel, Al-based alloys containing amorphous and nanocrystalline phases, Rev.Adv. Mater. Sci 18 (2008) 169–172 http://www.ipme.ru/e-journals/RAMS/no_21808/eckert.pdf.
[16] A.L. Greer, Partially or fully devitrified alloys for mechanical properties, Mater. Sci. Eng. A304-306 (2001) 68–72, https://doi.org/10.1016/S0921-5093(00)01449-0.
[17] M.A. Muñoz-Morris, S. Suriñach, M. Gich, M.D. Baró, D.G. Morris, Crystallization of a Al–4Ni–6Ce glass and its influence on mechanical properties, Acta. Mater. 51 (2003) 1067–1077, https://doi.org/10.1016/S1359-6454(02)00511-6.
[18] G. Abrosimova, A. Aronin, The increase of strength properties at nanocrystal formation, Mater. Letters 206 (2017) 64–66, https://doi.org/10.1016/j.matlet.2017.06.098.
[19] F. Meng, K. Tsuchija, Y. Yokoyama, Reversible transition of deformation mode by structural rejuvenation and relaxation in bulk metallic glass, Appl. Phys. Letters 101 (2012) 121914, , https://doi.org/10.1063/1.4753998.
[20] Y. Tong, T. Iwashita, W. Dmowski, Structural rejuvenation in bulk metallic glasses, Acta Mater 86 (2015) 240–246, https://doi.org/10.1016/j.actamat.2014.12.020.
[21] W. Dmowski, Y. Yokoyama, A. Chuang, Y. Ren, M. Umemoto, K. Tsuchiya, A. Inoue, T. Egami, Structural rejuvenation in a bulk metallic glass induced by severe plastic deformation, Acta Mater 58 (2010) 429–438, https://doi.org/10.1016/j.actamat.2009.09.021.
[22] Y. Tong, W. Dmowski, H. Bei, Mechanical rejuvenation in bulk metallic glass induced by thermo-mechanical creep, Acta Mater 148 (2018) 384–390, https://doi.org/10.1016/j.actamat.2018.02.019.
[23] W. Guo, R. Yamada, J. Saida, Rejuvenation and plasticization of metallic glass by deep cryogenic cycling, Intermetallics 93 (2018) 141–147, https://doi.org/10.

1016/j.intermet.2017.11.015.
[24] G. Abrosimova, N. Volkov, Tran Van Tuan, A. Aronin, Cryogenic rejuvenation of Al-based amorphous-nanocrystalline alloys, Mater. Letters. 240 (2019) 150–152, https://doi.org/10.1016/j.matlet.2018.12.131.
[25] S.V. Ketov, Y.H. Sun, S. Nachum, Z. Lu, A. Checchi, A.R. Beraldin, H.Y. Bai, W.H. Wang, D.V. Louzguine-Luzgin, M.A. Carpenter, A.L. Greer, Nature 524 (2015) 200–203, https://doi.org/10.1038/nature14674.
[26] T.C. Hufnagel, Cryogenic rejuvenation, Nat. Mater. 14 (2015) 87–88, https://doi.org/10.1038/nmat4394.
[27] G.E. Abrosimova, I.M. Shmytko, The use of single-crystal cuvettes with the properties of an optical shutter in X-ray diffractometers, Ind. Lab. Diagn. Mater. 84 (2018) 34–37, https://doi.org/10.26896/1028-6861-2018-84-6-34-37.
[28] T. Gloriant, M. Gich, S. Surinach, M.D. Baro, A.L. Greer, Evaluation of the volume fraction crystallized during devitrification of Al-based amorphous alloys, Mater. Sci Forum 343-346 (2000) 365–370 www.scientific.net/JMNM.8.365.
[29] H.W. Yang, J. Wen, M.X. Quan, J.Q. Wang, Evaluation of the volume fraction of nanocrystals devitrified in Al-based amorphous alloys, J. Non-Cryst. Solids 355 (2009) 235–238, https://doi.org/10.1016/j.jnoncrysol.2008.12.001.
[30] G.E. Abrosimova, A.S. Aronin, N.N. Kholstinina, On the determination of volume fraction of the crystalline phase in amorphous-crystalline alloys, Physics of the Solid State 52 (2010) 445–451, https://doi.org/10.1134/S1063783410030017.
[31] D.V. Louzguine-Luzgin, I. Seki, S.V. Ketov, L.V. Louzguina-Luzgina, V.I. Polkin, N. Chen, H. Fecht, A.N. Vasiliev, H. Kawaji, Glass-transition process in an Au-based metallic glass, J. Non Cryst. Solids 419 (2015) 12–15, https://doi.org/10.1016/j.jnoncrysol.2015.03.018.
[32] G. Abrosimova, D. Matveev, E. Pershina, A. Aronin, Effect of treatment conditions on parameters of nanocrystalline structure in Al-based alloys, Mater. Letters 183 (2016) 131–134, https://doi.org/10.1016/j.matlet.2016.07.053.
[33] A. Aronin, D. Matveev, E. Pershina, V. Tkatch, G. Abrosimova, The effect of changes in al-based amorphous phase structure on structure forming upon crystallization, J. All. Comp. 715 (2017) 176–183, https://doi.org/10.1016/j.jallcom.2017.04.305.
[34] Z. Wang, C.L. Chen, S.V. Ketov, K. Akagi, A.A. Tsarkov, Y. Ikuhara, D.V. Louzguine-Luzgin, Local chemical ordering within the incubation period as a trigger for nanocrystallization of a highly supercooled Ti-based liquid, Mater. Des. 156 (2018) 504–513, https://doi.org/10.1016/j.matdes.2018.07.013.
[35] P.R. Elliot Constitution of Binary Alloys, First Supplement, McGraw-Hill Book Company, NY, 1970, p. 472.
[36] G. Abrosimova, A. Aronin, D. Matveev, E. Pershina, Nanocrystal formation, structure and magnetic properties of Fe–Si–B amorphous alloy after deformation, Mater Lett 97 (2013) 15–17, https://doi.org/10.1016/j.matlet.2013.01.092.
[37] G. Abrosimova, A. Aronin, On decomposition of amorphous phase in metallic glasses, Rev. Adv. Mater. Sci 50 (2017) 55–61 http://www.ipme.ru/e-journals/RAMS/no_15017/07_15017_abrosimova.pdf.
[38] G. Abrosimova, A. Aronin, A. Budchenko, Amorphous phase decomposition in Al–Ni–Re system alloys, Mater Lett 139 (2015) 194–196, https://doi.org/10.1016/j.matlet.2014.10.076.
[39] A. Guinier, Theorie et technique de la radiocristallographie, Dumond, Paris, 1956.
[40] R.V. Sundeev, A.V. Shalimova, A. Glezer, J. All. Comp. 611 (2014) 292–296, https://doi.org/10.1016/j.jallcom.2014.05.109.
[41] R.V. Sundeev, A.V. Shalimova, A. Glezer, E.A. Pechina, M.V. Gorshenkov, Structural aspects of strain amorphization of a Ti50Ni25Cu25 crystalline alloy under high pressure torsion, Physics of the Solid State 60 (2018) 1168–1172, https://doi.org/10.1134/S106378341806032X.
[42] F.C. Serbena, E.D. Zanotto, Internal residual stresses in glass ceramics: a review, J. Non Cryst. Solids 358 (2012) 975–984, https://doi.org/10.1016/j.jnoncrysol.2012.01.040.
[43] Physical quantities. Handbook, in: I.S. Grigoryev, E.Z. Meilokhov (Eds.), Physical quantities. Handbook, Energoatomizdat, Moscow, 1991In Russian.
[44] G.H. Li, W.M. Wang, X.F. Bian, Correlation between thermal expansion coefficient and glass formability in amorphous alloys, Mater Chem Phys 116 (2009) 72–75, https://doi.org/10.1016/j.matchemphys.2009.02.041.
[45] L. Boichyshyn, V. Kovbuz, O. Hertsyk, V. Nosenko, B. Kotur, Influence of structurization of amorphous metallic alloys $Al_{87}Y_{5-x}Gd_xNi_{8-y}$ ($x = 0, 1, 5$; $y = 0, 4$) on their mechanical properties, Phys. Solid State 55 (2013) 243–246, https://doi.org/10.1134/S1063783413020054.
[46] G.E. Abrosimova, A.S. Aronin, Size effect on the structure of Al- and Ni-based nanocrystals, Phys. Solid State 50 (2008) 159–163, https://doi.org/10.1134/S1063783408010289.